SIMULATION OF THE EFFECTS OF HARD LIMITING ON IMAGE QUALITY OF SYNTHETIC APERATURE RADAR*

RICHARD G. LIPES and STANLEY A. BUTMAN
Caltech's Jet Propulsion Laboragory

Summary. Starting with a magnetic tape of a scene viewed by the ERTS (Landsat) satellite, we simulated the radar return of reflectors whose average intensity matched that of the picture elements in the scene. The returns were processed in three ways: normally or with no quantization, with a procedure simulating IF (intermediate frequency) hard limiting, and with a procedure simulating video (baseband) hard limiting. For each type of processing we developed an image for a one, two, and four-look system. We found that IF limiting is slightly better than video limiting, while both can be reasonable trade-offs of image quality for reduced data rates when the number of looks is four or less. These conclusions are supported by photographs representing the different processing techniques.

Introduction. Spacecraft synthetic aperature radar (SAR) (Refs. 1-3) mapping requires an enormous processing capability to achieve both the high resolution and wide coverage required by the user. At present this volume of processing, and the need for adaptability in case of spacecraft orbit and pointing anomalies, is approachable only by telemetry of the raw radar echo for processing on the ground. Therefore, the data rates required are in the 100 megabit per second range and some form of data rate reduction is desirable. When an on-board processor becomes feasible it may be possible to use the "usual" data compression techniques (removing scene redundancy), coupled with on-board storage to reduce the data rates to the Megabit per second region and below. However, since raw radar echoes from even adjacent resolution cells are essentially uncorrelated, redundancy removal is inapplicable and other methods must be found. The most promising method is to limit the digitization or quantization (bits per sample) of the raw echo prior to transmission.

The purpose of this article is to present the results of such quantization tradeoffs in the form of pictures of a photographic scene for the user community to evaluate.

*This paper presents the results of one phase of research carried out at the Jet Propulsion Laboratory, California Institute of Technology, under Contract No. NAS 7-100, sponsored by the National Aeronautics and Space Administration.

The idea to limit the quantization of the raw radar echo is not new. It has been actively pursued by developers of digital processors for SAR, but, much of the data is unpublished. The effect of limiting has also been investigated analytically, for example, by Sternberg (Ref. 4) and Zeoli (Ref. 5). Sternberg has shown that when the reconstruction of a reasonably homogeneous scene requires correlation of a large number of returns, hard limiting (1 bit quantization) of the returns hardly degrades the signal-to-noise ratio (SNR) of representative resolution cells. As expected, when the scene contains prominent specular returns, “false targets” or “ghosts” will be created by the nonlinear limiting process. Using a narrowband Gaussian process, Zeoli found that the distortion due to video limiting was only -8 db, and due to IF limiting, -9 db.

Since the user of an imaging radar system must judge the output image, we want to display the effects of limiting on the image itself. To this end we have chosen to simulate the raw radar return from a scene viewed by the ERTS (Earth Resources Technology Satellite) or Landsat satellite. In this way we have “ground truth” (exceedingly difficult information to obtain for actual radar data) for assessing the effects of limiting. The output takes form as pictures of fixed resolution representing radar images of varying numbers of looks obtained by processing with no limiting, IF limiting, or video limiting. These pictures can be compared with each other and “ground truth” to determine image quality and data rate reduction tradeoffs based on specific user need.

This study proceeds as follows. In Section II we discuss and analyze simulation of the raw radar return. We develop an expression for the complex return in terms of radar design parameters. This expression is used to determine the resolution capabilities of the system. The statistical properties of the return are assumed to arise from a Rayleigh scattering model since we have been primarily interested in the effects of limiting on images not possessing strong specular returns. Finally, we bring together these concepts to formulate our simulation model. In Section III we delineate the processing of the simulated radar return. First, we consider normal processing to obtain the best image possible for a given number of looks. Next we consider the two bandwidth compressing operations of IF limiting and video limiting to determine their effect on image quality relative to normal processing. In Section IV we discuss these results and draw conclusions concerning bandwidth compression and image degradation tradeoffs.

II. Analysis and Simulation. A. Radar Return

Suppose a single pulse f(t) with RF carrier frequency f_0, phase modulation $\phi(t)$ and duration Δ, is transmitted by the radar. The return from a point scatterer a distance r(t) away (in general this distance will vary with time when the radar and scatterer are in relative motion) will be of the form $\sigma f(t-\frac{2r(t)}{c})$. The round trip distance introduces a delay $\frac{2r(t)}{c}$ and causes an inverse fourth power attenuation in the complex constant σ

which represents the complex reflectivity of the scatterer. In the applications we are considering the fourth power attenuation is approximately the same for all points in the beam and will be ignored. Assume the radar is sidelooking and moving with constant velocity v as shown in Fig. 1. When the azimuth beamwidth is much less than the distance to the scatterer, assumed motionless, this distance can be approximated as

$$r(t) \approx r_a + \frac{(x_a - vt)^2}{2r_a} \tag{1}$$

where x_a is the azimuth or along flight path coordinate and r_a is the range or perpendicular to flight path coordinate of the scatterer. The return from a single pulse from a point scatterer is then

$$\sigma(x_a, r_a) \exp j \left[2\pi f_0 \left(t - \frac{2r_a}{c} - \frac{(x_a - vt)^2}{r_a c}\right) + \phi\left(t - \frac{2r_a}{c}\right) \right] \tag{2}$$

where $\sigma = \sigma(x_a, r_a)$ and we have assumed the azimuth beamwidth is sufficiently narrow so that $\phi(t)$ varies negligibly in time $(x_a - vt)^2 / (2r_a c)$ (notice this assumes range curvature is negligible). To form an image of a terrain the radar transmits a successive pulse every T seconds. By design, the distance it moves between pulses is less than or equal to its azimuthal resolution. Consequently, we can assume the azimuthal coordinate vt of the radar is nearly constant during the return from the n^{th} pulse, so $vt \approx x_n$. The total return to the radar, heterodyned to baseband, is obtained by superimposing the contribution from all scatterers in the beam:

$$g(x_n, r) \approx \sum_{x_a, r_a} \sigma(x_a, r_a) \exp j \left[-\frac{4\pi r_a}{\lambda} - \frac{2\pi}{r_a \lambda} (x_a - x_n)^2 + \phi\left(\frac{2}{c}(r - r_a)\right) \right] \tag{3}$$

where $\lambda = \frac{c}{f_0}$ is the carrier wavelength. The variable $r = \frac{ct}{2}$ indicates the maximum range of scatterers contributing to the return at time t. Notice that with our approximations $g(x_n, r)$ is expressed as a two-dimensional convolution over the range and azimuthal coordinates of the scatterers.

B. Resolution Capabilities

The range resolution capability depends upon the form of phase modulation function $\phi(t)$ that is employed. We will assume $\phi(t)$ is a “chirp” or linear FM waveform:

$$\phi(t) \equiv \begin{cases} \pi b t^2 & 0 \leq t \leq \Delta \\ 0 & \text{otherwise} \end{cases} \tag{4}$$

To recover the complex reflectivity $\sigma(x_a,r_a)$ we can correlate the return with reference function $\exp j\left[\frac{2\pi x^2}{r} - \phi(\frac{2r}{c})\right]$. The correlation $c(x,r)$ becomes

$$c(x,r) \equiv \int dx' \int dr'\ g(x+x', r+r')\ \exp j\left[\frac{2\pi x'^2}{\lambda r} - \phi(\frac{2r'}{c})\right] \approx$$

$$\begin{cases} \sum_{x_a,r_a} \sigma(x_a,r_a)\ \exp j\left[\frac{2\pi b\Delta}{c}(r-r_a) - \frac{4\pi r_a}{\lambda}\right] \frac{c^2}{4\pi b(r-r_a)}\ \sin\left[\frac{4\pi b}{c^2}(r-r_a)(\frac{c\Delta}{2} - |r-r_a|)\right] \\ \qquad \times \quad \frac{r\lambda}{2\pi(x-x_a)}\ \sin\left[\frac{2\pi(x-x_a)}{r\lambda}\ (L_A - |x-x_a|)\right] \\ \qquad\qquad\qquad\qquad \text{for } |r-r_a| < \frac{c\Delta}{2},\ |x-x_a| < \frac{L_A}{2} \\ 0 \qquad\qquad \text{otherwise} \end{cases}$$

where we have approximated the sum over azimuth coordinates as an integral and have introduced the azimuth beamwidth L_A. The sum over r_a, x_a receives significant contributions only from scatterers satisfying $|r-r_a| \leq \frac{c}{2b\Delta}$ when $b\Delta^2 >> 1$ and $|x-x_a| \leq \frac{r\lambda}{2L_A}$ when $2L_A^2/r\lambda >> 1$. Since the azimuth beamwidth L_A is related to the radar antenna azimuth dimension D_A by $L_A \approx \frac{r\lambda}{D_A}$ the latter condition becomes $|x-x_a| \leq \frac{D_A}{2}$ when $2L_A/D_A >> 1$. The correlation effectively partitions the radar image into a grid of resolution cells of widths $\frac{c}{2b\Delta}$ in range and $D_A/2$ in azimuth.

C. Statistical Properties of the Return

The actual radar return will be composed of a specular scattering component and a Rayleigh scattering component with their relative importance being determined by the composition of the area being illuminated and the orientation of its scatterers relative to the radar. The processing techniques to be discussed in Section III will distort the image of the illuminated area. The general features of the specular component have been previously investigated (Ref. 4) so in this work we will be concerned only with the distortion of the Rayleigh component. Therefore, we will restrict ourselves to scattering that is Rayleigh in nature and assume the diffuse scattering surface is rough on the scale of the carrier wavelength λ (Refs. 6,7). From eq. (5) we see that the correlation (x,r) is reasonably well approximated by

$$c(x,r) \approx k \frac{c\Delta L_A}{2} \sum_{x_a,r_a}{}' \sigma(x_a,r_a) \exp -j \left[\frac{4\pi r_a}{\lambda}\right] \quad (6)$$

where $\sum'$ signifies summation over the resolution cell centered at (x,r) and k is a constant of order unity.

Since $r >> \lambda$, when the resolution cell contains a large number of scatterers, the summation can be viewed as the addition of independent random variables of the form $pe^{j\theta}$ where θ is a random variable uniform on $[0, 2\pi]$. From the assumption of a small specular component we have no appreciable variation in the complex reflectivity over a resolution cell so ρ is nearly constant. Finally, invoking the central limit theorem, we can model the return from a resolution cell as a zero mean complex Gaussian random variable whose real and imaginary parts are statistically independent identically distributed with variance proportional to the mean power return from the cell. Furthermore, the returns from different resolution cells are statistically independent.

D. Simulation Model

Our model to simulate SAR operation now takes conceptual form as follows. We partition the scene of interest into a grid of resolution cells and assume the mean power return from each cell is known. This defines the image whose facsimile we will recover after simulation and processing. For each resolution cell we generate two identically distributed statistically independent zero mean Gaussian random variables with variance equal to one half the mean power of the cell. These form the real and imaginary parts of the complex reflectivity of the cell and represent the term $\sigma(x_a,r_a)$ exp-j $[4\pi r_a/\lambda,]$ of Eq. (3) where (x_a,r_a) now corresponds to the coordinates of the resolution cell. To complete the simulated radar return we carry out the two dimension range and azimuth convolution as indicated in Eq. (3).

Starting with a magnetic tape of a scene viewed by the ERTS or Landsat satellite shown in Fig. 5, we simulated the radar return of reflectors whose ensemble mean intensity matched that of the picture elements (pixels) in the scene. The scene consists of 256 by 256 pixels. We assumed the radar had a pulse repetition frequency equal to the Nyquist rate of the azimuth or Doppler return and the echo was sampled at the Nyquist rate of $\phi(t)$ of Eq. (4). Therefore, the return of Eq. (3) was formed from superimposing single complex samples from each of 60762 contributing resolution cells, since the radar modeled had azimuth and range time-bandwidth products (TBP's) of N_A= 247 and N_R =246 respectively. These TBP's represented a compromise between the quite large TBP's of satellite SAR's and the feasible number of computer operations involved in simulating and processing a 256 by 256 pixel picture. The raw return to resolution cell labeled by in azimuth and range by ℓ_A

and ℓ_R respectively takes form as a digitized version of Eq. (3):

$$g(\ell_A,\ell_R) = \sum_{m_A,m_R} \delta(m_A,m_R)\ \exp j\pi\left\{(\ell_R-m_R)^2/N_R-(\ell_A-m_A)^2/M(\ell_R)\right\} \tag{7}$$

where $\delta(m_A,m_R)$ is the complex sample from the (m_A,m_R) resolution cell. $M(\ell_R)$ accounts for the range dependence of the Doppler phase. If the ratio of range resolution to slant range is γ, then $M(\ell_R) = N_A(1+ \gamma\ell_R)$. We used $\gamma= 10^{-5}$ as representative of satellite SAR's.

The preceding discussion treats the return as a complex quantity, whereas, in implementing the simulation, we must deal with the real and imaginary parts. A block diagram of the radar return simulation is shown in Fig. 2. The real part is labeled with an I (in-phase) and the imaginary part is labeled with Q (quadrature). The row and column convolutions are performed by fast Fourier transform (FFT) (Ref. 8) techniques because of the computational time savings they afford.

III. Processing. As explained in the preceding section, the complex reflectivity from a resolution cell is obtained by correlating the radar return with the appropriate reference function. The square of the magnitude of the complex reflectivity is then displayed to form the output image for a single look. A block diagram of the procedure is seen in Fig. 3. As in simulation, the correlations are implemented using FFT techniques.

A. Processing Strategies

Also, shown in Fig. 3 is a box labeled "Processing Selection". We have investigated three types of processing strategies:

1. Normal Processing. By normal processing we mean that the baseband radar return is passed directly into the processor with no intermediate and possibly degrading operations performed on it. This mode represents the highest quality in output image that can be obtained for a single look system of given resolution.

2. IF Limiting. The return to the radar is, of course, riding on the RF carrier at frequency f_0. Normally, this signal is heterodyned to an intermediate frequency (IF) before being mixed and low-pass-filtered to baseband. We wished to investigate the degradation that would occur if hard limiting was applied to the IF signal. Since the mixing and low-pass-filtering operations that occur after the IF stage allow complete recovery of the phase of the IF signal before hard limiting (Ref. 9), we can simulate IF limiting by normalizing the amplitudes of all the returns to the same value while leaving the phase unchanged. This process is represented by the phasor diagram in Fig. 4. The amplitude normalized signals are then passed to the processor.

3. Video Limiting. Finally, we wished to investigate the degradation resulting from hard limiting the baseband radar returns. These returns exist in the form of I (in-phase) and Q (quadrature) components so we hard-limited the two components separately. As shown in Fig. 4 this restricts the amplitude of all returns to the same value and permits only four phase values $\pm \frac{\pi}{4}, \pm \frac{3\pi}{4}$. Notice this baseband or video limiting is more severe than the IF limiting which causes no phase distortion.

B. Multiple Looks

As stated in the discussion of the statistical properties of the radar returns, in the Rayleigh model both I and Q components are statistically independent identically distributed zero mean Gaussian random variables with variance proportional to the mean power return from a resolution cell. This means the sum of squares of the I and Q components or intensity of the return is an exponentially distributed random variable whose mean is the mean power return from the resolution cell. Since the mean power from a resolution cell is the quantity of interest in forming an image of the scene, we need to estimate it from the intensities we obtain from independent single "looks". Clearly, the sample mean formed from independent intensities provides the best estimate of the ensemble mean. The difference in the sample mean and ensemble mean gives rise to the characteristic "speckle" of images formed from coherent illumination (Refs. 10-14). In this work we have formed sample means for 1, 2, and 4 independent intensities or looks. In displaying the images for 1, 2, and 4 looks we have kept the resolution cell size fixed for the following reason. Suppose the user is interested in detecting a small feature of the scene viewed by the radar whose area corresponds to 10-15 resolution cells. The amount of "speckle" in the image is critically important in determining whether such a feature can be reliably identified: it may be possible to identify a feature in a four-look image that is lost in the speckle of a one-look image. Consequently, the images we present allow the user to determine for a given resolution the number of looks (between 1 and 4) necessary to identify specific scene characteristics. We are certainly aware that in an actual radar system there is a trade-off between number of looks and effective resolution, but if too few looks are obtained detailed features of considerable interest may be lost in the speckle.

IV. Results and Conclusions. We processed the simulated raw radar data with no further degradation, with IF limiting, and with video limiting to obtain single-look images. From independent generation of random variables in the simulation procedure, we developed three additional independent single-look images for each processing strategy. Averages of one, two, and four of these single-look images were made corresponding to one-, two-, and four-look systems. Again, we emphasize in actual radar applications increasing the number of looks requires sacrificing resolution since registration problems

prevent averaging as described above. The results are shown in Fig. 6. All pictures have been normalized so that the average intensity is constant.

It is immediately apparent that none of the pictures representing ≤ 4 looks are close in clarity to the "ground truth" of Fig. 5. Speckle severely limits their clarity causing a "graininess" that is reduced only by increasing the number of looks. As expected, for fixed number of looks the IF and video limited pictures are inferior to the normally processed one. However, certain details of the 2-look and 4-look limited pictures are correspondingly absent in the respective 1-look and 2-look normal ones. It appears that limiting "costs" somewhat less than a look, so some users may tolerate the image quality degradation of limiting to realize an important data rate reduction. Finally, we compare IF limiting with video limiting. Since the two limiting procedures differ only in less phase distortion with IF limiting, it must produce a more faithful output. From the pictures of Fig. 6 it is qualitatively difficult to discern this, although IF limiting may appear slightly better.

REFERENCES

1. Cutrona, L. J., Leith, E. N., Porcello, L. J., and Vivian, W. E., "On Application of Coherent Optical Processing Techniques to SyntheticAperature Radar", Proc. of IEEE, Vol. 54, No. 8, 1026 (1966).
2. Brown, W. M.,"Synthetic Aperature Radar", IEEE Transactions on Aerospace and Electronic Systems, Vol. AES-3, Noi 2, 217 (1967).
3. Skolnik, M. I., Editor, "Radar Handbook", McGraw-Hill Book Co., (1970) Chapter 23, "Synthetic Aperature Radar" (Cutrona, L. J.)
4. Sternberg, B. D., "Hard Limiting in Synthetic Aperature Signal Processing", IEEE Transactions on Aerospace and Electronic Systems, Vol. AES-11, No. 4, 556 (1975).
5. Zeoli, G. W., "IF Versus Video Limiting for Two-Channel Coherent Signal Processors", IEEE Transactions on Information Theory, Vol. IT-17, No. 5, 579 (1971).
6. Beckman, P. and Spizzichino, A., "The Scattering of Electromagnetic Wave from Rough Surfaces", MacMillian Co., New York, (1963).
7. Lord Rayleigh, "The Theory of Sound", MacMillian Co. 3rd Edition, London (1896).
8. Rabiner, L. R. and Rader, C. M. editors, "Digital Signal Processing," Part 2-The Fast Fourier Transform, IEEE Press, New York, (1972).
9. Davenport, W. B., and Root, W. L., "Random Signals and Noise", Chapter 13, MacGraw-Hill Book Co., New York (1958).
10. Schiffner, G., "Granularity in the Angular Spectrum of Scattered Laser Light", Proc. of IEEE, Vol. 53, 1245 (1965).
11. Enloe, L. H., "Noise-Like Structure in the Image of Diffusely Reflecting Objects in Coherent Illumination", Bell Systems Tech. J., Vol. 46, 1479 (1967).
12. Gabor, D., "Laser Speckle and Its Elimination", IBM J. Theo. Develop. Vol. 14, 509

(1970).
13. Mitchell, R. L., “Models of Extended Targets and Their Coherent Radar Images,” Proc. of the IEEE, Vol. 62, No. 6, 754 (1974).
14. Butman, S., and Lipes, R. G., “The Effects of Noise and Diveristy on Synthetic Array Radar Imagery”, in Deep Space Network Progress Report 42-29, Jet Propulsion Laboratory, Pasadena, California, p. 46, July and August 1975.

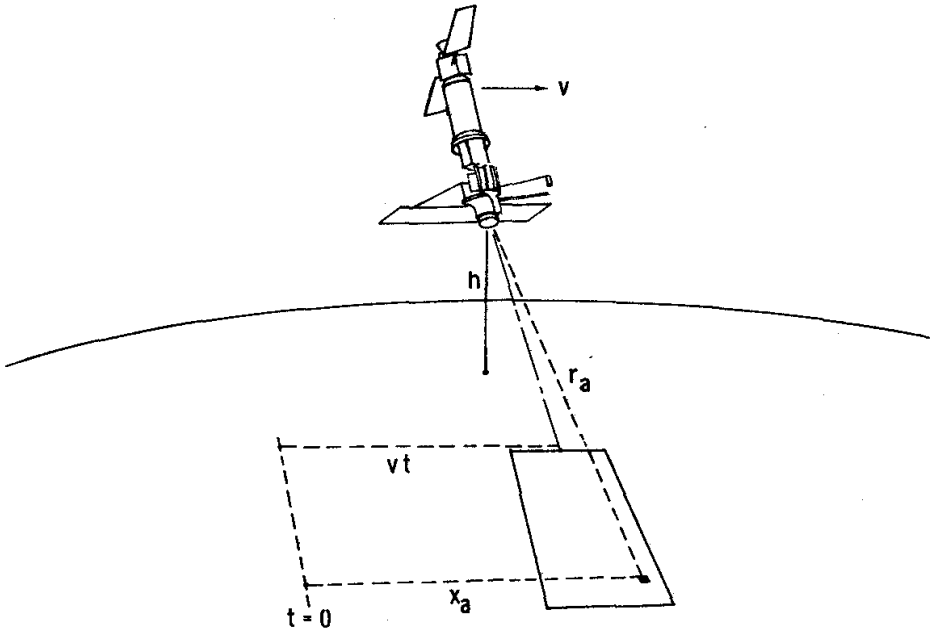

Satellite SAR geometry showing location of point scatterer at (x_a, r_a)

Fig. 1

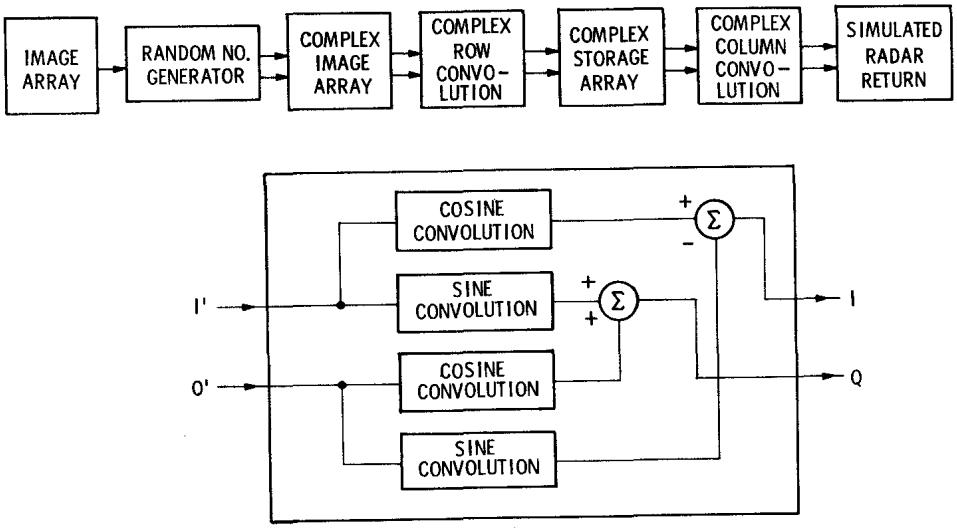
IMAGE ARRAY
RANDOM NO. GENERATOR
COMPLEX IMAGE ARRAY
COMPLEX ROW CONVO-LUTION
COMPLEX STORAGE ARRAY
COMPLEX COLUMN CONVO-LUTION
SIMULATED RADAR RETURN
COSINE CONVOLUTION
SINE CONVOLUTION
COSINE CONVOLUTION
SINE CONVOLUTION
I'
Q'
I
Q
COMPLEX ROW / COLUMN CONVOLUTION
Block diagram of Radar Simulation

Fig. 2

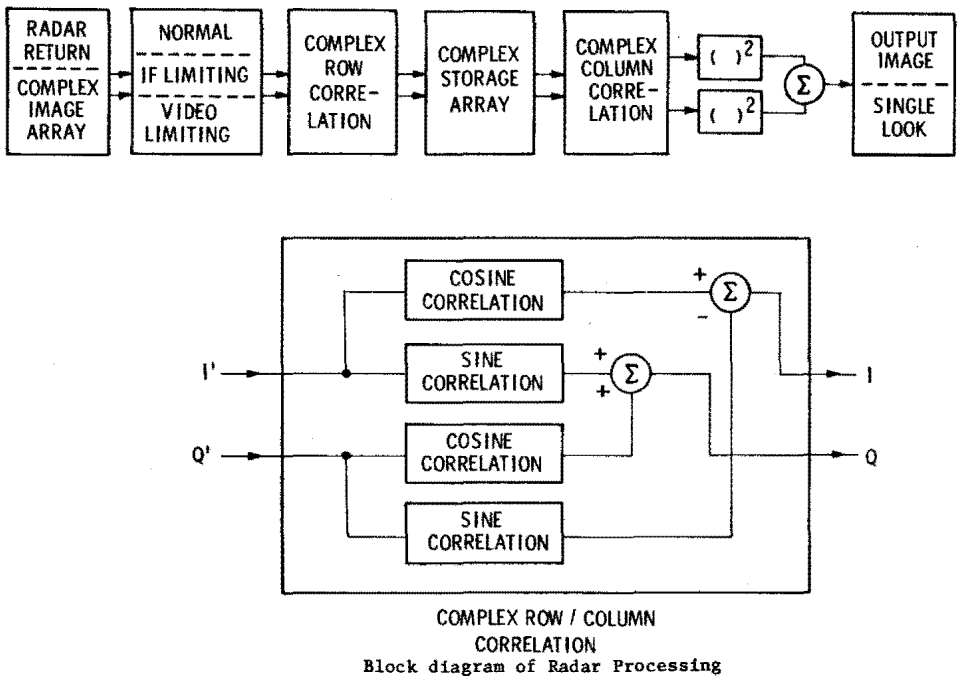
RADAR RETURN
COMPLEX IMAGE ARRAY
NORMAL
IF LIMITING
VIDEO LIMITING
COMPLEX ROW CORRE-LATION
COMPLEX STORAGE ARRAY
COMPLEX COLUMN CORRE-LATION
OUTPUT IMAGE
SINGLE LOOK
COSINE CORRELATION
SINE CORRELATION
COSINE CORRELATION
SINE CORRELATION
I'
Q'
I
Q
COMPLEX ROW / COLUMN CORRELATION
Block diagram of Radar Processing

Fig. 3

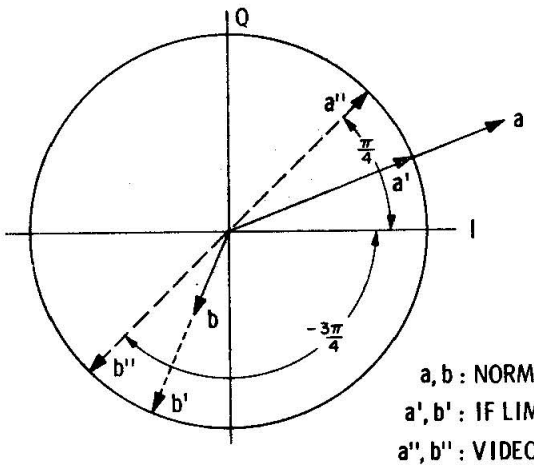

Phasor diagram showing effects of IF and video limiting on normal returns.

Fig. 4

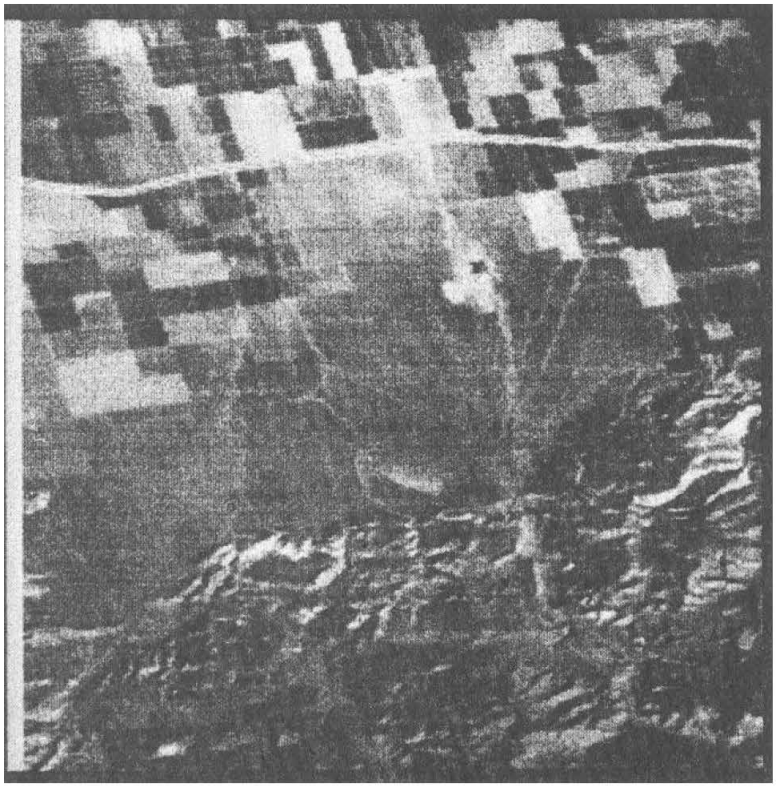

Scene from ERTS or Landsat satellite used as input to radar simulation

Fig. 5

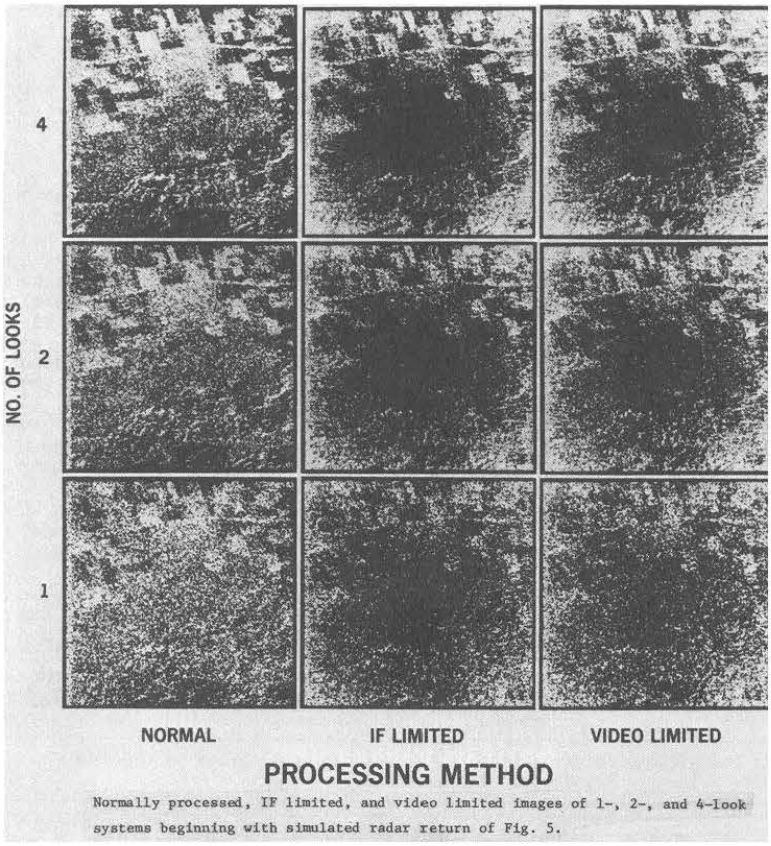

Normally processed, IF limited, and video limited images of 1-, 2-, and 4-look systems beginning with simulated radar return of Fig. 5.

Fig. 6